



**HAL**  
open science

## Simulations for Tuning a Laser Power Control System of the Cladding Process

Piotr Jurewicz, Wojciech Rafajlowicz, Jacek Reiner, Ewaryst Rafajlowicz

► **To cite this version:**

Piotr Jurewicz, Wojciech Rafajlowicz, Jacek Reiner, Ewaryst Rafajlowicz. Simulations for Tuning a Laser Power Control System of the Cladding Process. 15th IFIP International Conference on Computer Information Systems and Industrial Management (CISIM), Sep 2016, Vilnius, Lithuania. pp.218-229, 10.1007/978-3-319-45378-1\_20 . hal-01637520

**HAL Id: hal-01637520**

**<https://inria.hal.science/hal-01637520v1>**

Submitted on 17 Nov 2017

**HAL** is a multi-disciplinary open access archive for the deposit and dissemination of scientific research documents, whether they are published or not. The documents may come from teaching and research institutions in France or abroad, or from public or private research centers.

L'archive ouverte pluridisciplinaire **HAL**, est destinée au dépôt et à la diffusion de documents scientifiques de niveau recherche, publiés ou non, émanant des établissements d'enseignement et de recherche français ou étrangers, des laboratoires publics ou privés.



Distributed under a Creative Commons Attribution 4.0 International License

# Simulations for Tuning a Laser Power Control System of the Cladding Process

Piotr Jurewicz<sup>1</sup>, Wojciech Rafajłowicz<sup>2</sup>, Jacek Reiner<sup>1</sup>, and Ewaryst Rafajłowicz<sup>2</sup>

<sup>1</sup> Wrocław University of Science and Technology, Faculty of Mechanical Engineering, Wrocław, Poland, [jacek.reiner@pwr.edu.pl](mailto:jacek.reiner@pwr.edu.pl)

<sup>2</sup> Wrocław University of Science and Technology, Faculty of Electronics, Wrocław, Poland, [ewaryst.rafajlowicz@pwr.edu.pl](mailto:ewaryst.rafajlowicz@pwr.edu.pl)

**Abstract.** Our aim is present the methodology of simulations for repetitive processes and tuning control systems for them in the presence of noise. This methodology is applied for tuning a laser power control system of the cladding process. Even the simplest model of this process is nonlinear, making analytical tuning rather difficult. The proposed approach allows us to select quickly the structure of the control system and to optimize its parameters. Preliminary comparisons with experimental results on a robot-based laser cladding systems are also reported. These comparisons are based on the temperature measurements, observations by a camera and IR camera.

**Keywords:** control system, simulations, IR camera, laser cladding

## 1 Introduction

Additive manufacturing for building (or printing) 3D structures, e.g., laser cladding process is apparently one of the most promising cost and time intensive technologies. A laser power control is a crucial factor for the high quality of the cladding process (see [13]). Other factors that influence building a 3D body from a melted powder include the powder supply rate and the velocity of the laser head movements. The process is so complicated that several models of it have been proposed (see, e.g., [8], [6]), but even the simplest of them – adopted from [13] also in this paper – is described by a nonlinear differential equation, which has to be extended by adding differential equations of a controller and a filter. Thus, the proper selection of the control system structure and tuning of its parameters requires extensive simulations, because direct experiments on a real systems are forbidden as being dangerous – the laser power is about 1 kW. The construction of the robot that performs movements of the laser head is shown in Fig. 1 (left panel), while the right panel shows the laser head with a camera that looks at the cladding process along the laser beam. Notice that in [1] an original, alternative construction that is specifically designed station, which is based on a three-axis CNC machine equipped with the laser head. The results presented in this paper are expected to be useful also for this new construction.

Our aim in this paper is to propose a methodology for running such simulations. The needs for an extension of control systems simulations methodology stems from the following features of the laser cladding:

- the process is a repetitive one, i.e., the laser heating head moves back and forth when developing a 3D object (see [12] for a review of repetitive processes and their applications),
- radiation/optical sensors (e.g. camera, pyrometer) or thermovision – infrared camera can be used for the process monitoring,
- the repetitive process is time-varying between the passes of the laser head (see the right panel in Fig. 2, where the temperature of a hot, melted metal lake is gradually growing from pass to pass).

Notice that similar features are present in 3D printers and in other additive, powder based technologies, which can make the methodology proposed here more universal.

From the view-point of the designing a control system our in this paper goals are the following:

1. to tune parameters of the PI controller so as to minimize a control quality criterion that is specific for the laser power control task, namely, we penalize too large jumps of the laser power,
2. to decide whether a filter that makes the control signal smoother should be used or not.

The reason for considering the second goal is in extremely large variations in measurements of the lake temperature. This fact can be seen in Fig. 2 (right panel), in which one can observe spikes that differ by  $\pm 50$ -100 degrees from the mean temperature of the surroundings, while typical errors are at the levels  $\pm 20$ . These errors are caused either by image processing, since it is very difficult to locate the the hottest place of the lake (see Fig. 2 – left panel) or by a pyrometer that averages the lake temperature, but at the turning points it averages partly the lake temperature and partly the temperature of the surrounding (see [3] for extensive investigations of cladding process by IR camera). One can expect that such a filter will act also as an anti-wind up module (see, e.g., [7] for practical explanations of wind-up phenomenon in control systems with PI controllers). The paper is organized as follows. In the next section we describe the models of:

- the dependence of the lake temperature on the laser power,
- proportional-integral (PI) controller,
- control signal smoothing module

and the methodology of simulations is presented. Then, we use this methodology to reach the two goals mentioned above. Finally, we present an excerpt of the results obtained from experimental implementation of the proposed control system.

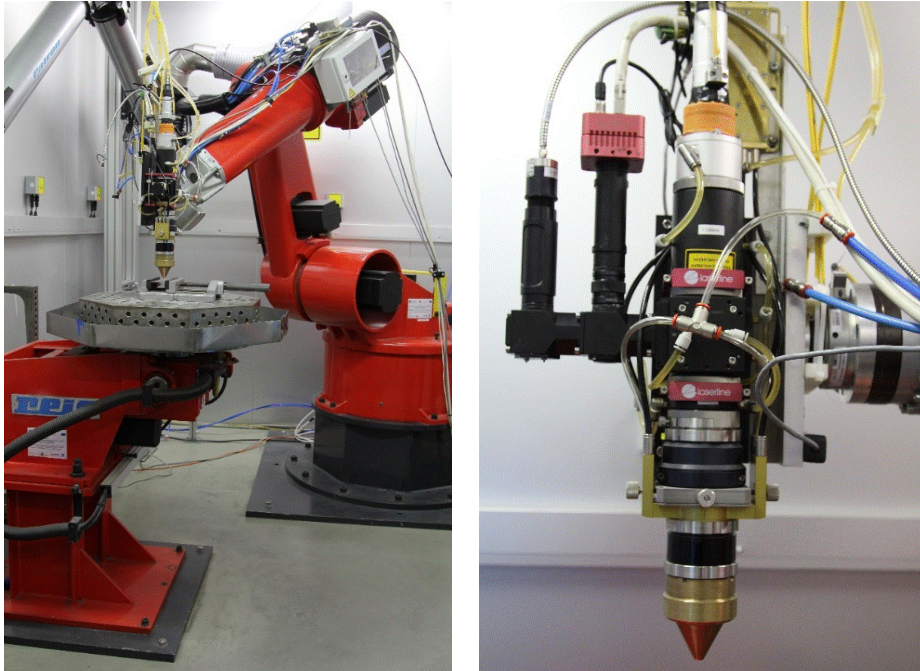


**Fig. 1.** Cladding robot (left panel) and the laser head with a camera (right panel)

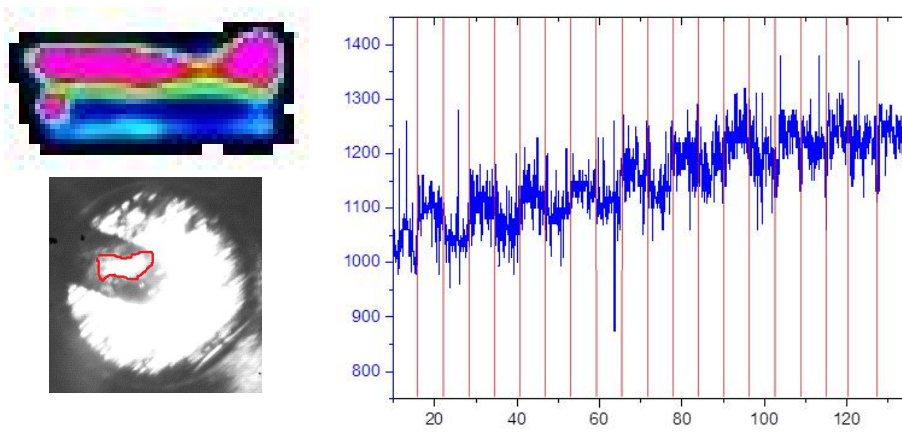


**Fig. 2.** Left panel – image of the first cladding pass with the lake marked (lower left panel) and IR image of the lake (upper left panel). Temperatures of the lake – several cladding passes (right panel)

## 2 Laser Power Control – Model and Simulation Methodology

A mathematical model for one laser pass of the dependence between the laser power  $Q(t)$  and the lake temperature  $y(t)$  has been adapted from the paper of Tang and Landers Part I [13] (later abbreviated as TL). It has the following form:

$$\tau y'(t) + y(t) = K (Q(t))^\beta, \quad y(0) = y_0 \quad (1)$$

where  $y_0$  - given initial temperature. The constants in (1) are defined as follows (compare [13]):

- $\beta = 6.25 \cdot 10^{-2}$  is an experimentally selected constant,
- $\tau = 2.96 \cdot 10^{-2}$  - in sec. is the system time constant.

Overall system gain  $K$  (amplification) is defined by

$$K = K_1 (V^\alpha) (M^\gamma) = 1413.58, \quad (2)$$

where:

- $K_1 = 0.5 \cdot 10^3 \cdot 1.42 \cdot 10^3$  is empirically established system amplification,
- $V = 3.4$  in mm/sec is the laser traverse speed,
- $M = 4.0$  in g/min - the powder supply rate,
- $\alpha = -7.1 \cdot 10^{-3}$  and  $\gamma = 3.0 \cdot 10^{-3}$  experimentally selected constants.

In [5] a more exact nonlinear model for the lake temperature is derived that takes into account also the laser head position. One can incorporate this model in our simulation methodology, replacing (1) by the model from [5]. However, model (1) occurred to be sufficiently exact for a constant speed of the laser head, since then  $t$  simultaneously specifies the head position.

For a multi-pass cladding process we have to extend model (1) by including the heat exchange between passes. We propose the simplest model that can incorporate the influence of the temperature at  $k$ -th pass  $y_k(t)$  on the temperature at  $(k + 1)$  pass, i.e.,  $y_{k+1}(t)$  of the following form: for passes  $k = 0, 1 \dots$

$$\tau y'_{k+1}(t) + y_{k+1}(t) = K (W_{k+1}(t))^\beta + \xi y_k(t), \quad y_{k+1}(0) = Y_k(0), \quad t \in (0, T), \quad (3)$$

where  $T > 0$  is the pass length (the time that the laser head needs to travel along a 3D object under construction),  $W_k(t)$  is the laser power at  $k$ -th pass at time  $t$ , while  $\xi$  is the coefficient that governs the influence of the temperature at  $k$ -th pass, denoted as  $Y_k(t)$ , on the lake temperature at the next pass. Due to forth and back movements of the laser head, for  $t \in [0, T]$   $Y_k(t)$  is defined as follows:

$$Y_k(t) = \begin{cases} y_k(t) & \text{if } k \text{ odd,} \\ y_k(T - t) & \text{if } k \text{ even.} \end{cases} \quad (4)$$

In order to run (3) we need also the initial condition along the pass, which is assumed to be  $Y_0(t) = Y_0 = \text{const}$ ,  $t \in [0, T]$ , where  $Y_0$  is the temperature of the base.

To check model (3), it was run with a constant laser power  $W = 0.2$  kW. The results are shown in Fig. 3. Comparing it to Fig. 2 (right panel) one can

observe similar qualitative behavior, i.e., the lake temperature grows from pass to pass, and then it stabilizes at the level of about 1250-1300° C. Notice that in Fig. 3 the temperatures from subsequent passes are tilled, while in Fig. 2 they are joined serially.

The analysis of Fig. 2 reveals why a control system for the lake temperature stabilization is necessary. Namely, at the points where the laser head turns back one can observe the essential growth of the lake temperature, since at a short time the laser operates twice at the same regions, near the end points. In [7] the proportional-integral (PI) controller is proposed, together by an anti-wind-up by the feedback from the saturation block to the input of PI controller. The control system scheme that is proposed in this paper is depicted in Fig. 4. It consists of PI-controller followed by a control signal smoothing module. The PI-controller that is usually described as follows:

$$q(t) = K \left( e(t) + \frac{1}{T_i} \int_0^t e(\tau) d\tau \right), \quad (5)$$

where  $K > 0$  is the amplification,  $T_i > 0$  is the time of doubling of the error signal  $e(t)$ , while  $q(t)$  is the controller output. For the purposes of our simulations it is convenient to rewrite (5) as follows:

$$q_k(t) = K_P e_k(t) + K_I \int_0^t e_k(\tau) d\tau, \quad (6)$$

where  $K_P > 0$  is the amplification of P-that,  $K_I > 0$  is the amplification of I-path,  $e_k(t) = y_{ref}(t) - y_k(t)$  is the tracking error at  $k$ -th pass and  $y_{ref}(t)$  is the reference signal, which is assumed to be constant<sup>3</sup> in this paper. The integral term in (6) reduces the tracking error and reduces the laser power variability. However, due to large measurement errors, this reduction is not sufficient. For this reason, the control smoothing exponentially weighted moving average (CSEWMA) filter is added in the control loop (see Fig. 4). In fact, CSEWMA is a low pass filter with a specific parametrization that allows its intuitive tuning (see [10]). Being the low-pass filter, CSEWMA acts also as an anti-wind-up device by reducing large changes of the laser power. For our purposes the CSEWMA filter is described as follows:

$$W_k'(t) = -h W_k(t) + h q_k(t), \quad W_k(0) = W_k^0, \quad (7)$$

where  $W_k^0$  is defined as

$$W_k^0 = \begin{cases} W_{k-1}(0) & \text{if } k \text{ odd,} \\ W_{k-1}(T) & \text{if } k \text{ even.} \end{cases}, \quad (8)$$

while  $0 < h < 1$  is a smoothing parameter. Its role is easy to interpret when a finite difference approximation is considered:

$$W_k(t + \Delta t) = (1 - h \Delta t) W_k(t) + h \Delta t q_k(t). \quad (9)$$

<sup>3</sup> It is reasonable to consider also time-varying  $y_{ref}(t)$  so as to compensate a shape of 3D body at the laser turning points, but the discussion on this is outside the scope of our paper.

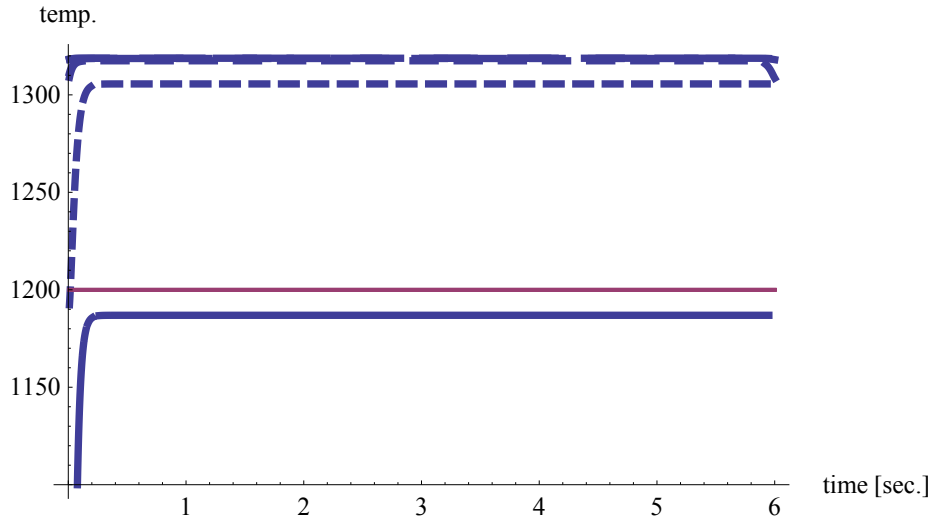


**Fig. 3.** The results of pass-to-pass simulations – the lake temperature growth from pass 1 (solid curve) through pass 2 (the shortest dashed line) to pass 4 (the longest dashed line). The solid straight line – the desired temperature of the lake

Hence, the output of the filter at  $t + \Delta t$  is a weighted combination of its older output  $W_k(t)$  and its input  $q_k(t)$ . Smaller values of  $h$  force more smoothing.

**Algorithm 1 – algorithm for simulating a repetitive control system.**

**Step 0)** Select  $K_P > 0$ ,  $K_I > 0$ ,  $0 < h < 1$ ,  $y_{ref}(t)$  and the number of passes  $kmax$ . Set pass counter  $k = 1$  and  $Y_0(t) = Y_0$ ,  $t \in [0 T]$ .

**Step 1)** Solve the following system of coupled differential and integral equations for  $t \in (0, T)$

$$\tau y'_k(t) + y_k(t) = K (W_{k+1}(t))^\beta + \xi Y_{k-1}(t), \quad y_{k+1}(0) = Y_k(0), \quad (10)$$

$$q_k(t) = K_P (y_{ref}(t) - y_k(t)) + K_I \int_0^t (y_{ref}(\tau) - y_k(\tau)) d\tau, \quad (11)$$

$$W'_k(t) = -h W_k(t) + h q_k(t), \quad W_k(0) = W_k^0. \quad (12)$$

**Step 2)** Update  $Y_k(t)$  and  $W_k^0$  according to, (4) and (8), respectively. If  $k < kmax$ , set  $k := k + 1$  and go to Step 1), otherwise, STOP.

Several remarks are in order concerning the above algorithm.

1. The pass index  $k$  is used for  $y_k(t)$ ,  $W_k(t)$  and  $q_k(t)$  for readability. However, in the implementation it suffices to store only four lists that contain the

- sampled versions of current  $W_k(t)$  and  $q_k(t)$  as well as sampled versions of  $y_{new}(t)$  and  $y_{old}(t)$  to store the sampled versions of  $y_k(t)$  and  $y_{k-1}(t)$ , respectively, and then to change the contents of  $y_{old}(t)$  by  $y_{new}(t)$  at Step 2.
2. The algorithm has been extensively tested by the authors. The excerpt of the results is shown in Fig. 6.
  3. A general construction of the algorithm is applicable for simulating repetitive control systems for other processes. To this end, it suffices to replace (10) by another one (or by the set of differential equations).
  4. The control system in Algorithm 1 is nonlinear. However, the static nonlinearity is rather weak and for verifying the system stability along the pass we can use the results form [12], Chapter 7.5 for a linearized system.

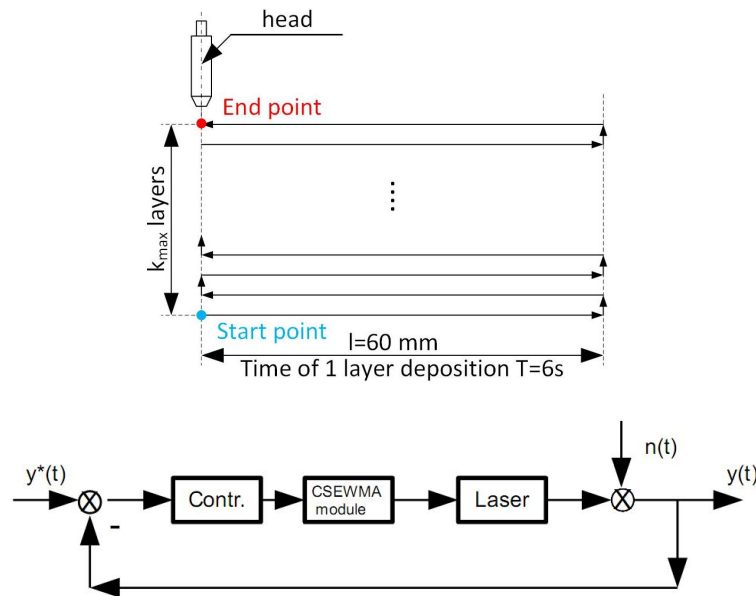


**Fig. 4.** Upper panel – the scheme of laser cladding as a repetitive process. Lower panel – a closed loop system with a controller combined with the CSEWMA module – control along the pass

### 3 Tuning the Control System by Simulations

Our aim in this section is to propose the methodology of running simulations for tuning the control system, i.e., selecting parameters of PI controller and CSEWMA block.



A control quality index  $J(K_I, h, D)$  depends on parameter  $K_I$  of PI controller, parameter  $h$  of CSEWMA block and on  $kmax \times N$  matrix  $D$  of observation errors. This matrix consists of rows  $\bar{d}^{(k) \text{ def}} [d_1^{(k)}, d_2^{(k)}, \dots, d_N^{(k)}]$ , where  $d_n^{(k)}$ 's are realizations of independent random variables with zero mean and a probability distribution selected by the user. For  $J(K_I, h, D)$  we propose to take the following expression:

$$\begin{aligned} J(K_I, h, D) &= \\ &= \Delta \sum_{n=1}^N |y_{ref}(t_n) - \hat{y}_{kmax}(t_n, d_n)| + \gamma \Delta \sum_{n=2}^N |W_{kmax}(t_n) - W_{kmax}(t_{n-1})|, \end{aligned} \quad (13)$$

where  $\Delta > 0$  is the sampling period ( $N \Delta = T$ ),  $\gamma > 0$  is the weight of the second penalty term, while  $\hat{y}_{kmax}(t_n, d_n)$  is defined as

$$\hat{y}_{kmax}(t_n, d_n^{(kmax)}) = y_{kmax}(t_n) + d_n^{(kmax)}, \quad n = 1, 2, \dots, N, \quad (14)$$

where  $y_{kmax}(t_n)$  is obtained from the last pass of Algorithm 1 at  $n$ -th sampling instant. Notice that  $\hat{y}_{kmax}(t_n, d_n^{(kmax)})$  indirectly depend on all earlier realizations of random errors, since in Algorithm 1 we use the following expression:

$$\hat{y}_k(t) = K_P (y_{ref}(t) - \hat{y}_k(t)) + K_I \int_0^t (y_{ref}(\tau) - \hat{y}_k(\tau)) d\tau, \quad (15)$$

instead of (11), with obvious changes also in (12). In (15)  $\hat{y}_k(t)$  is a noise corrupted version of  $y_k(t)$  that is obtained as follows: after calculating  $y_k(t)$  (by solving (10)) this signal is sampled and corrupted by random disturbances:

$$\hat{y}_k(t_n, d_n^{(k)}) = y_k(t_n) + d_n^{(k)}, \quad n = 1, 2, \dots, N. \quad (16)$$

Then,  $\hat{y}_k(t)$  is obtained by interpolating  $\hat{y}_k(t_n, d_n^{(k)})$ .

The first term in (13) is the mean absolute deviation of the system output from the reference value. The second term in (13) is less obvious in control theory. It is a penalty for too large changes in a control signal, i.e., the laser power in our case. Notice that this term is similar to, but not the same as, the total variation, which is the norm in the space of functions with bounded variation (see, e.g., [2] for the definition and properties.).

Taking into account that  $D$ 's is randomly generated, we have to average  $J(K_I, h, D)$  also with respect to  $D$ . The following algorithm calculates the averaged quality index for fixed  $K_I$  and  $h$

$$\tilde{J}(K_I, h) = j_{max}^{-1} \sum_{j=1}^{j_{max}} J(K_I, h, D^{(j)}), \quad (17)$$

where  $D^{(j)}$  is  $j$ -th realization of random matrix  $D$ ., while  $j_{max}$  is the number of samples used for averaging.

**Algorithm 2** – algorithm for estimating quality of a repetitive control system for fixed tuning parameters.

**Step 0)** Select  $K_P > 0$ ,  $K_I > 0$ ,  $0 < h < 1$ ,  $y_{ref}(t)$  and the number of repetitions  $j_{max}$ . Set run counter  $j = 1$  and  $S = 0$ .

**Step 1)** Generate a random matrix  $D^{(j)}$  and use its elements in (16).

**Step 2)** Run Algorithm 1 with (15) replaced by (11).

**Step 3)** Calculate  $J(K_I, h, D^{(j)})$  according to (13) and update  $S = S + J(K_I, h, D^{(j)})/j_{max}$ .

**Step 4)** If  $j < j_{max}$ , set  $j := j + 1$  and go to Step 1). Otherwise, STOP with  $S$  as the output.

Having Algorithm 2 at our disposal we can optimize  $\tilde{J}(K_I, h)$  with respect to  $K_I$  and  $h$  (and possibly other parameters of the control system). To this end, one can use one of many available and well known global optimization algorithms, e.g., genetic or evolutionary algorithms (see, e.g., [4]) or their recently developed versions that take constraints into account by applying the Fletcher filter [9], [11]. The need for using global optimization methods instead of faster but local ones stems from the fact that random errors may lead to false local minima, even if a large number of repetitions  $j_{max}$  is used.

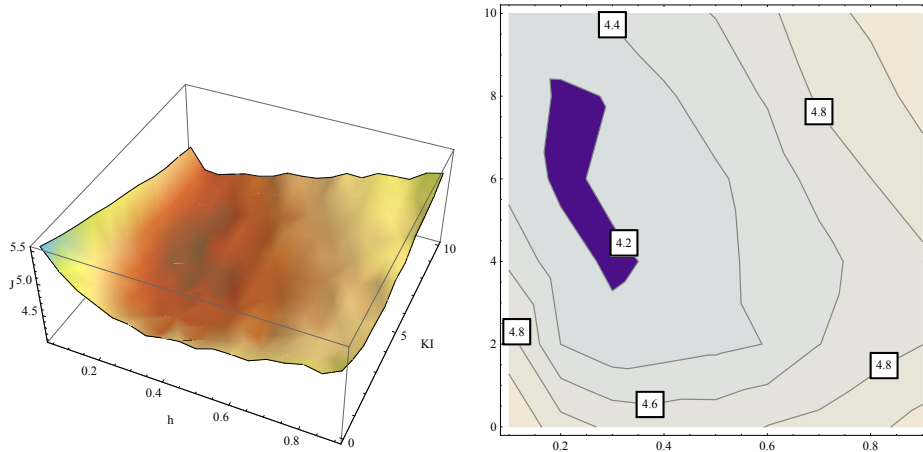


**Fig. 5.** Dependence of control quality criterion  $\tilde{J}(K_I, h)$  on  $(K_I$  and  $h$  – 3D plot (left panel) and contour plot (right panel)

The time of running Algorithm 2 once, for 6 cladding layers and  $j_{max} = 600$  repetitions, was about 100 sec. on a standard PC i7/3 GHz. In order to grasp an intuition how the landscape of  $\tilde{J}(K_I, h)$  looks like, Algorithm 2 has been run on

the grid for  $h \in [0.1, 0.9]$  and  $K_I \in [0, 10]$ . The remaining parameters have been selected as follows:  $K_P = K_E = 1$ ,  $\Delta = 0.01$  sec., random errors – uniformly distributed in  $[-20, 20]$  °C. The results of the simulations are shown in Fig. 5. As one can notice, the landscape is rather flat, but the global optimum is clearly visible. Although a relatively large number of repetitions  $j_{max} = 600$  has been used, one can find many local minima (see, e.g., a vicinity of  $h = 0.85$ ,  $K_I = 5$  – left panel of Fig. 5). Nevertheless, for the right panel of this figure, one can easily read out that pairs  $(h, K_I)$  in the darkest region provide the smallest  $\tilde{J}(K_I, h)$ , which is equal to 4.2. The larger region:  $h \in [0.2, 0.55]$ ,  $K_I \in [3.5, 8]$  provides quite good quality of about 4.4. Thus, the cladding process can be run safely in this region.

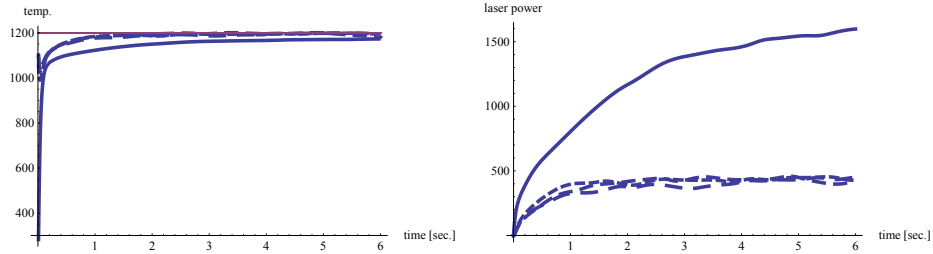


**Fig. 6.** Four passes of the cladding process for approximately optimal tuning of the control system. Left panel – the lake temperature vs time. Right panel – the laser power used

## 4 Selected Experimental Results

The results presented in the previous sections have been based on simulations. Here, we provide selected experimental results of using the PI-CSEWMA control system to the laser cladding robot. A 3D thin wall has been built several times, using different settings of the control system that are listed in the first and the second column in Table 1. The third column contains  $J$  criterion, as defined by (13), with  $\lambda = 3$  and  $\Delta = 1/6$ . The reason for selecting this value is the following: the length of each pass was 6 seconds, but for evaluating  $J$  we have taken 2000 samples (from 5000 to 7000) in the middle of the pass, which corresponds to one second. The results displayed in the fourth column is the percentage of the improvement of  $J$  by introducing control systems in comparison to the case when constant power  $\bar{W} = 0.65$  kW was applied (first row). As one can observe, introducing the PI controller reduces  $J$  by 38 %. Additional reduction, by additional 14 % is obtained when under-smoothed ( $h = 0.5$ ) CSEWMA filter is introduced. When properly selected smoothing ( $h = 0.1$ ) in CSEWMA filter is applied, then we obtain the reduction of  $J$  to 65 – 66 % of its value without control. Notice that interchanging positions of PI and CSEWMA smoother does

Control syst.	Param.	$J = \text{eq.}(13)$	% improv.
none (const. W)	–	8.25	–
PI	$K_P = 0.9, K_I = 5.88$	5.13	38
PI+CSEWMA 1	$K_P = 0.9, K_I = 5.88, h = 0.5, q_0 = 0$	3.95	52
PI+CSEWMA 2	$K_P = 0.9, K_I = 5.88, h = 0.1, q_0 = 0$	2.88	65
PI+CSEWMA 3	$K_P = 0.9, K_I = 5.88, h = 0.1, q_0 = 450$	2.81	66
CSEWMA + PI	$K_P = 0.9, K_I = 5.88, h = 0.1, q_0 = 0$	2.78	66

**Table 1.** The quality of control (3-rd column) for different control system configurations and tuning (1-st column) and the percentage of the improvement with respect to no control (constant laser power) case (4-th column)

not influence this result. Applying other than zero initial state of CSEWMA filter also does not improve the performance, although it can be desirable in order to get even smoother control signals.

## 5 Conclusions and the Directions ff Further Research

The methodology of simulating the dynamics of controlled repetitive processes and optimizing parameters of the control system has been presented in details. Then, this methodology has been applied to the laser power control of the cladding process. The control system consisting of PI-controller and CSEWMA filter has been tuned by the simulations. Then, the designed control system has been tested on a real-life cladding robot. The results are satisfactory in the sense that we have obtained a good performance of the system both in its pass-to-pass behavior as well as in its behavior along each pass, which is smoother then in the case when the CSEWMA filter is not used.

Further effort is needed to better control the material deposition at the end points, using images from the IR (thermvision camera), but this topic is outside the scope of this paper.

## References

1. Baraniecki, T., Chlebus, E., Dziatkiewicz, M., Kędzia, J., Reiner, J., Wiercioch, M.: System for laser microsurfacing of metal powders. *Welding International* 30(2), 98–102 (2016)
2. Benedetto, J.J., Czaja, W.: *Integration and modern analysis*. Springer Science & Business Media (2010)

3. Bi, G., Gasser, A., Wissenbach, K., Drenker, A., Poprawe, R.: Investigation on the direct laser metallic powder deposition process via temperature measurement. *Applied Surface Science* 253(3), 1411–1416 (2006)
4. Coello, C.A.C., Van Veldhuizen, D.A., Lamont, G.B.: *Evolutionary algorithms for solving multi-objective problems*, vol. 242. Springer, Heidelberg (2002)
5. Devesse, W., De Baere, D., Guillaume, P.: Design of a model-based controller with temperature feedback for laser cladding. *Physics Procedia* 56, 211–219 (2014)
6. Liu, J., Li, L.: Effects of process variables on laser direct formation of thin wall. *Optics & Laser Technology* 39(2), 231–236 (2007)
7. Mandarapu, S., Lolla, S., Kumar, M.S.: Digital pi controller using anti-wind-up mechanism for a speed controlled electric drive system. *International Journal of Innovative Technology and Exploring Engineering (IJITEE)*, ISSN pp. 2278–3075 (2013)
8. Picasso, M., Marsden, C., Wagniere, J., Frenk, A., Rappaz, M.: A simple but realistic model for laser cladding. *Metallurgical and materials transactions B* 25(2), 281–291 (1994)
9. Rafajłowicz, E., Rafajłowicz, W.: Fletchers filter methodology as a soft selector in evolutionary algorithms for constrained optimization. In: *Swarm and Evolutionary Computation*, In: Leszek Rutkowski, Marcin Korytkowski, Rafa Scherer, Ryszard Tadeusiewicz, Lotfi A. Zadeh, Jacek M. Zurada (eds), pp. LNCS, vol. 7269, pp. 333–341. Springer, Heidelberg (2012)
10. Rafajłowicz, E., Wnuk, M., Rafajłowicz, W.: Local detection of defects from image sequences. *International Journal of Applied Mathematics and Computer Science* 18(4), 581–592 (2008)
11. Rafajłowicz, W.: Numerical optimal control of integral-algebraic equations using differential evolution with fletchers filter. In: *Artificial Intelligence and Soft Computing*. In: L. Rutkowski et al (eds.). pp. LNCS vol. 8467 pp. 406–415. Springer, Heidelberg (2014)
12. Rogers, E., Galkowski, K., Owens, D.H.: *Control systems theory and applications for linear repetitive processes*, vol. 349. Springer Science & Business Media (2007)
13. Tang, L., Landers, R.G.: Melt pool temperature control for laser metal deposition processespart i: Online temperature control. *Journal of manufacturing science and engineering* 132(1), 011010 (2010)

**Acknowledgements.** The works of Piotr Jurewicz, Jacek Reiner and Ewaryst Rafajłowicz have been supported by the National Science Center under grant: 2012/07/B/ST7/01216, internal code 350914 of the Wrocław University of Science and Technology. Wojciech Rafajłowicz has been supported by the Grant B50328 for Young Researchers from the Faculty of Electronics, Wrocław University of Science and Technology 2015/016.